

Visible-Light Azidation and Chemical Patterning of Graphene via Photoredox Catalysis

Published as part of *The Journal of Physical Chemistry virtual special issue "Early-Career and Emerging Researchers in Physical Chemistry Volume 2"*.

Wan Li,[†] Yunqi Li,[†] Bowen Wang, and Ke Xu*

Cite This: *J. Phys. Chem. C* 2022, 126, 21281–21286

Read Online

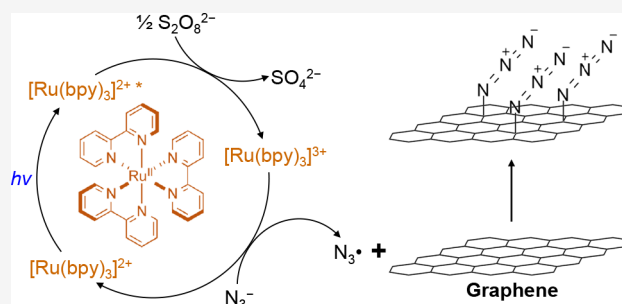
ACCESS |

Metrics & More

Article Recommendations

Supporting Information

ABSTRACT: We report a photocatalytic approach for the facile azidation and chemical patterning of graphene. Employing the classic photoredox catalyst tris(bipyridine)ruthenium(II) chloride, $[\text{Ru}(\text{bpy})_3]\text{Cl}_2$, azidyl radicals are generated in an aqueous solution of sodium azide under low illumination of blue light, e.g., filtered out from a white lamp. The photogenerated azidyl radicals efficiently azidate monolayer graphene, and the resultant azidated graphene further enables chemically defined derivations through click chemistry and subsequent bioconjugation. By controlling the illumination pattern in the wide field, we further demonstrate the direct photopatterning of graphene functionalization with low light, removing the need to focus an intense laser beam into a tight spot.



INTRODUCTION

Whereas chemical modifications offer great promise for expanding the functionalities and potential applications of graphene,^{1–12} the chemical inertness of the basal plane limits the available reaction approaches. Spatial patterning of chemical modifications^{13–27} presents yet another level of challenge. Radical reactions provide key routes to graphene functionalization.^{1,2,5,8} Our recent work has shown that in aqueous solutions, free radicals electrochemically generated at the graphene surface permit efficient reactions.^{28–30} In particular, in aqueous NaN_3 solutions, electrochemically generated azidyl radicals ($\text{N}_3\cdot$) effectively azidate monolayer graphene, hence providing a versatile product that enables chemically defined derivations through click chemistry and subsequent bioconjugation.²⁹

Here we report a facile, aqueous solution-based photosensitized pathway for graphene azidation, which removes the need to wire up graphene for electrochemistry while further enabling chemical patterning with low-intensity visible light.

Although free radicals generated from photodissociation have proved valuable for graphene reactions, surface depositions, and patterning,^{15,17,21–24,31–34} high-power illumination is often required to activate the reactants. Limited choices are available based on the optical absorptions and chemical activities of the specific reactants, and it is often difficult to further convert the functionalized graphene to other chemically defined surface functionalizations.

To achieve efficient photoreaction with visible light and, specifically, to remove one electron from aqueous-phase N_3^- to produce $\text{N}_3\cdot$ for graphene azidation and the ensuing versatile click chemistry, we consider single-electron-transfer photosensitizers. To this end, photoredox catalysis, e.g., with tris(bipyridine)ruthenium(II) chloride, $[\text{Ru}(\text{bpy})_3]\text{Cl}_2$, has in recent years emerged as a powerful tool in organic synthesis for driving radical reactions with visible light.^{35–37} A critical comparison has recently been made between reactions due to photoredox catalysis and electrochemistry,³⁸ and the generation of nitrogen-centered radicals by photoredox catalysis has been reviewed.³⁹ Yet, we are unaware of prior attempts to employ photoredox catalysis to activate aqueous N_3^- anions or to initiate other reactions for graphene and like nanomaterials.

MATERIALS AND METHODS

Photocatalytic Azidation of Graphene. Monolayer graphene grown on copper foils⁴⁰ (ACS Material or Graphene Supermarket) was wet-transferred through a modified RCA cleaning process⁴¹ onto #1.5 glass coverslips as $\sim 5 \times 10$ mm pieces. The sample was mounted on a standard inverted wide-

Received: October 21, 2022

Revised: November 18, 2022

Published: December 7, 2022



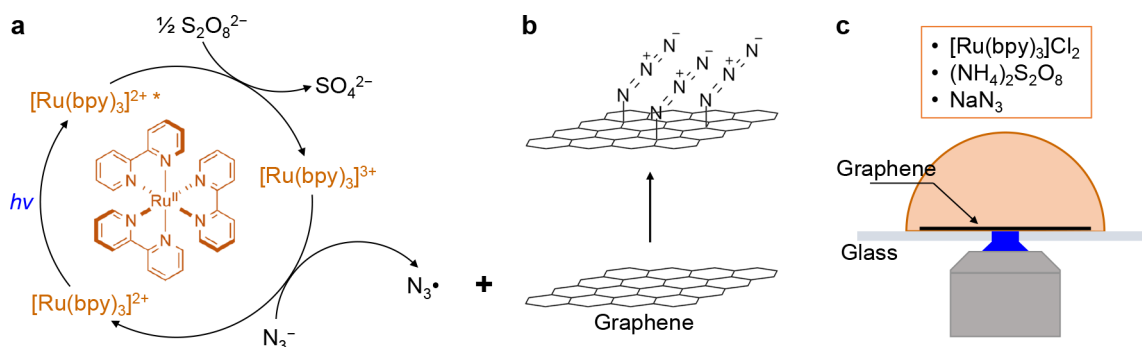


Figure 1. Schematics. (a, b) Reaction mechanisms: (a) Blue light excites $[\text{Ru}(\text{bpy})_3]^{2+}$ into a triplet excited state $[\text{Ru}(\text{bpy})_3]^{2+*}$, which readily loses one electron to peroxodisulfate to generate the highly active oxidant $[\text{Ru}(\text{bpy})_3]^{3+}$. $[\text{Ru}(\text{bpy})_3]^{3+}$ oxidizes N_3^- in the solution to azidyl radical ($\text{N}_3\cdot$) and returns to the starting $[\text{Ru}(\text{bpy})_3]^{2+}$. (b) The photogenerated $\text{N}_3\cdot$ reacts with graphene to produce azidated graphene. (c) Experimental setup: a drop of aqueous solution containing $[\text{Ru}(\text{bpy})_3]\text{Cl}_2$, $(\text{NH}_4)_2\text{S}_2\text{O}_8$, and NaN_3 is deposited on graphene on a glass coverslip. A region of the sample is evenly illuminated with blue light of preset patterns in the wide field through a microscope objective lens.

field epifluorescence microscope (Olympus IX73). Then, 0.1 mM $[\text{Ru}(\text{bpy})_3]\text{Cl}_2$ (Sigma 224758), 200 mM ammonium persulfate (Alfa Aesar 54106), and 200 mM NaN_3 (Sigma 71289) were dissolved in a 15 mM, pH = 7 phosphate buffer. An $\sim 100 \mu\text{L}$ drop of this solution was cast on the graphene surface. A standard filter cube on the Olympus IX73 microscope selected blue light from a white lamp (Olympus U-HGLGPS) and introduced it into the objective lens to illuminate a wide field of the sample. The filter cube was commonly used for the fluorescence imaging of Green Fluorescent Protein (GFP). With an excitation filter of ET470/40 \times (Chroma) and a dichroic mirror of T495lpxr (Chroma), the select-passed wavelength range was ~ 450 – 490 nm. When a low-magnification UPlanFL N 4 \times objective lens was used, a sample area of ~ 3 mm diameter was evenly illuminated. When an UplanFL 100 \times oil-immersion objective lens was used, a sample area of $\sim 50 \mu\text{m}$ diameter was evenly illuminated, with the actual illumination region defined by the adjustable field diaphragm of the microscope. The total illumination power was measured using a photodiode power sensor (S120VC, Thorlabs). By controlling the output level of the U-HGLGPS lamp source (3–25%) and using additional neutral-density filters (Thorlabs), the typical illumination power density at the sample was set to $\sim 10 \text{ mW}/\text{cm}^2$ ($\sim 0.1 \text{ nW}/\mu\text{m}^2$), as discussed in the main text. After the reaction, the sample was rinsed with 18 M Ω Milli-Q water and dried in air.

XPS Characterization. XPS was performed using a PerkinElmer PHI 5600 XPS instrument that was operated at $\sim 10^{-9}$ Torr with a monochromatic Al K α (1486.8 eV) X-ray source. A neutralizer was used to discharge accumulated charges from the sample surface. Element compositions were determined from the peak areas using the factory-calibrated relative sensitivity factors.

Cycloaddition and Subsequent Biotin–Streptavidin Conjugation of Azidated Graphene. A 0.02 mg sample of ADIBO–PEG $_4$ –biotin (Sigma-Aldrich 760749) was dissolved in 500 μL of 0.1 M potassium phosphate buffer (pH = 7). This solution reacted with both the azidated and control graphene samples in the dark for 1 h. The sample was rinsed with a 0.1 M potassium phosphate buffer three times and then treated with 3% bovine serum albumin (BSA; Sigma-Aldrich A3059) in Dulbecco's phosphate-buffered saline (DPBS; Corning 21-031-cv) for 30 min. Alexa Fluor 555-conjugated streptavidin (Invitrogen S21381) was constituted as a 2 mg/mL stock solution in DPBS. Two microliters of this solution was added

to 400 μL of DPBS containing 3% BSA, and the mixed solution was dropped onto the graphene sample. After 1 h of incubation in the dark, the sample was rinsed with DPBS 3 times and then rinsed with Milli-Q water and dried in air.

Optical Microscopy Characterizations. Fluorescence microscopy and interference reflection microscopy (IRM)⁴² were performed on an Olympus IX73 inverted epifluorescence microscope using an Olympus UplanFL 100 \times oil-immersion objective (numerical aperture ~ 0.9 with an iris diaphragm). For fluorescence microscopy of the labeled Alexa Fluor 555-conjugated streptavidin, the excitation filter, dichroic mirror, and emission filter were ET545/25 \times , zt561rdc-UF1, and ET605/70m, respectively (Chroma). For IRM, the excitation filter was D532/10 \times (Chroma), the dichroic mirror position was a 50/50 beam splitter (Chroma 21000), and the emission filter position was left empty.

Chemical Patterning through Patterned Illumination in the Wide Field. The graphene sample on the glass coverslip was mounted on a home-built super-resolution microscopy system based on a Nikon Eclipse Ti-E inverted fluorescence microscope.⁴³ The illumination source was a 488 nm laser (Coherent Sapphire), which was first passed through an acousto-optic tunable fiber (Gooch & Housego, 97-03151-01) for controlling the illumination power before being coupled into a single-mode optical fiber. Output from the fiber was expanded into a collimated beam ~ 20 mm in diameter and focused to the back focal plane of the objective lens (Nikon CFI Plan Apochromat λ 100 \times) using a lens of 40 cm focal length (2 \times of the tube-lens focal length), thus evenly illuminating a wide field $\sim 100 \mu\text{m}$ in diameter. A printed photomask (Outputcity) was placed at the expanded collimated beam that entered the microscope, so that the printed patterns were projected to the sample plane at a 200-fold size reduction. The same photocatalytic reactant solution as above was cast on the graphene surface, and the patterned illumination was applied for 15 min at a power density of $\sim 100 \text{ mW}/\text{cm}^2$ ($\sim 1 \text{ nW}/\mu\text{m}^2$) for the lower absorbance of $[\text{Ru}(\text{bpy})_3]\text{Cl}_2$ at 488 nm.

RESULTS AND DISCUSSION

In aqueous solutions, $[\text{Ru}(\text{bpy})_3]^{2+}$ exhibits a broad absorption band centered at ~ 450 nm (blue light) due to metal-to-ligand charge transfer. In the presence of a sacrificial oxidant such as peroxodisulfate, the resultant triplet excited state loses an electron to yield the potent oxidant $[\text{Ru}(\text{bpy})_3]^{3+}$ (Figure 1a).

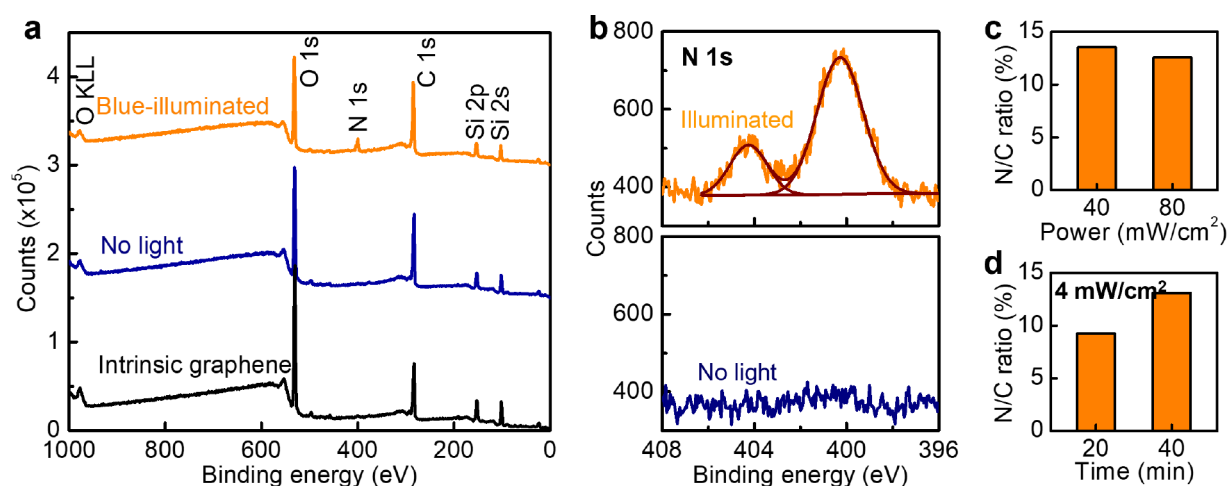


Figure 2. Effective photocatalytic azidation of graphene. (a) Survey-mode XPS results of monolayer graphene on glass substrates, before (back curve) and after (orange curve) 15 min of 40 mW/cm² blue-light illumination in the reactant solution, versus a control sample immersed in the same reactant for 15 min without illumination (blue curve). (b) High-resolution nitrogen 1s XPS for the illuminated and control samples. (c, d) XPS-determined N:C atomic ratios for two samples illuminated for 15 min at 40 and 80 mW/cm² (c) and for two other samples illuminated at 4 mW/cm² for 20 and 40 min (d), respectively.

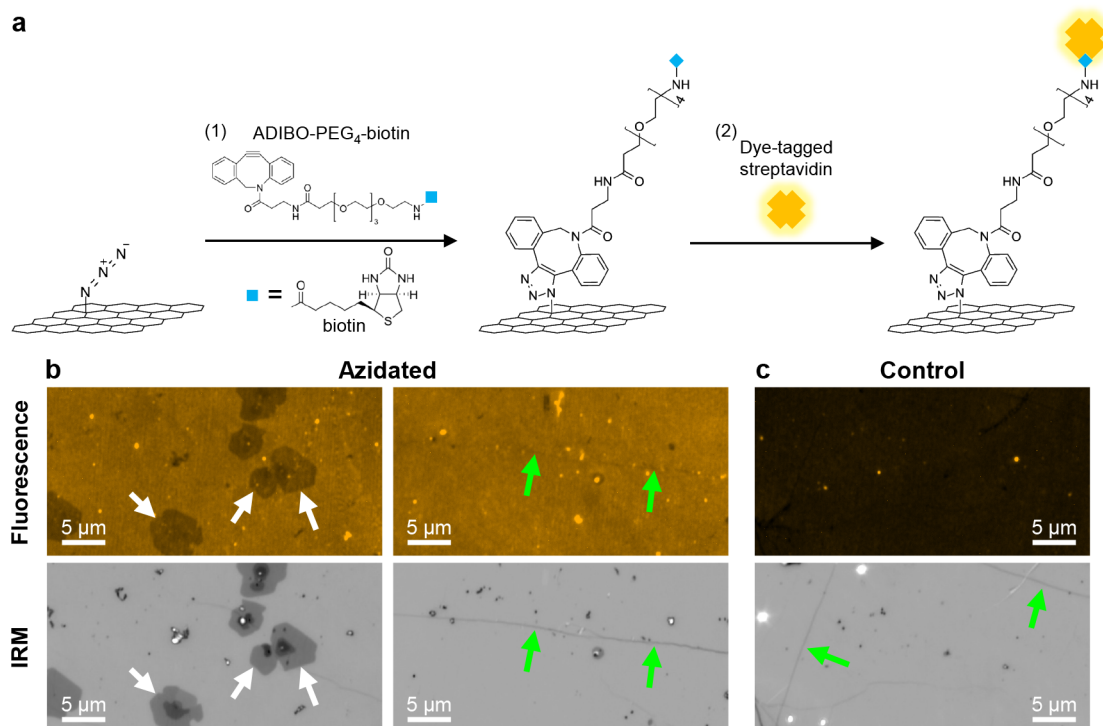


Figure 3. Click chemistry and bioconjugation of the photoazidated graphene. (a) Schematics: (1) Copper-free cycloaddition with azadibenzocyclooctyne (ADIBO)–PEG₄–biotin. (2) The functionalized biotin is next conjugated with fluorescently labeled streptavidin. (b) Fluorescence micrographs of the labeled streptavidin (top) and corresponding IRM images (bottom) of the final product. White and green arrows in (b) respectively point to occasionally observed bilayer islands and wrinkles in the monolayer graphene, where reduced fluorescence was observed. (c) Results on a control graphene sample that was not azidated but went through the same labeling process in (a). Green arrows point to wrinkles in the monolayer graphene.

We reason that in an aqueous solution of NaN₃, [Ru(bpy)₃]³⁺ may oxidize the azide anion N₃[−] to produce the azidyl radical N₃[•] (Figure 1a). Indeed, one early study has examined the equilibrium between the [Ru(bpy)₃]³⁺/[Ru(bpy)₃]²⁺ and N₃[•]/N₃[−] redox pairs, in which N₃[•] was generated through radiolysis.⁴⁴ The same equilibrium should be established if [Ru(bpy)₃]³⁺ is instead generated from the above photosensitization process. The resultant azidyl radicals may azidate

graphene (Figure 1b), as we have demonstrated with electrochemistry.²⁹

Monolayer graphene was deposited on glass substrates and mounted on a standard inverted wide-field epifluorescence microscope. [Ru(bpy)₃]Cl₂ was dissolved at 0.1 mM in a pH = 7 aqueous buffer containing 200 mM ammonium persulfate and 200 mM NaN₃. A small drop of this reactant solution was cast on the graphene surface. Using a standard filter cube, blue

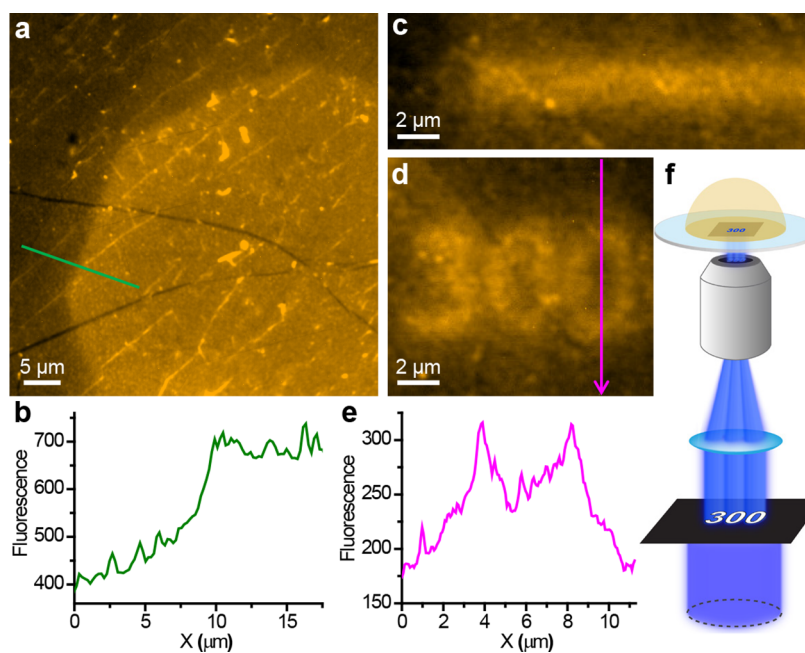


Figure 4. Chemical patterning of graphene functionalization via patterned illumination in the wide field. (a) Fluorescence micrograph of a sample after regional photocatalytic azidation and subsequent click chemistry and conjugation with dye-labeled streptavidin. Regional illumination was achieved with the field diaphragm of the microscope. (b) Fluorescence intensity profile along the green line in (a), crossing the boundary of the patterned azidation. (c, d) Patterning micrometer features as a straight line (c) and the text “300” (d). (e) Fluorescence intensity profile along the magenta arrow in (d). (f) Schematic: Defining desired illumination patterns in the wide field by inserting a printed photomask into the expanded illumination beam before the objective lens.

light was selected from a white lamp and introduced into the objective lens to illuminate the sample in the wide field at low power densities of ~ 10 mW/cm² (Figure 1c). Starting with a 4 \times low-magnification objective lens, we evenly illuminated an area of ~ 3 mm diameter, which was well-suited for the X-ray photoelectron spectroscopy (XPS) characterization of the product. Notably, the illumination led to the visible formation of bubbles: similar behavior has been noted in the electrochemical azidation of graphene,²⁹ suggesting the generation of excessive azidyl radicals, which self-combine to form N₂ gas ($2\text{N}_3 \cdot \rightarrow 3\text{N}_2$).

Figure 2a shows the XPS result of a sample that was illuminated at 40 mW/cm² for 15 min (orange curve). Notably, when compared to the untreated graphene (black curve), as well as a control sample that was immersed with the same reactant in the dark (blue curve), a substantial nitrogen 1s peak emerged in the illuminated sample. Examination of the high-resolution spectra (Figure 2b) showed two peaks at 400.3 and 404.3 eV at a $\sim 2:1$ ratio, in agreement with our previous results of azidated graphene and markedly different from the starting NaN₃.²⁹ Quantification of the XPS peak areas yielded an N:C ratio of 13.5% (Figure 2c), close to that achieved through electrochemistry.²⁹ Interference reflection microscopy (IRM)^{42,45} and Raman spectroscopy indicated enhanced doping with no significant defect generation after photocatalytic azidation (Figure S1), and electrical measurements showed increased conductivity consistent with enhanced doping (Figure S2). These results are also in line with what we previously observed with electrochemically azidated graphene.²⁹ As additional controls, we further examined samples that underwent the same illuminations in solutions without ammonium persulfate or [Ru(bpy)₃]Cl₂ and observed no noticeable azidation (Figure S3). Together, these results

indicate the successful photocatalytic azidation of graphene through our proposed pathway (Figure 1a and b).

Reducing the power density to 4 mW/cm² still permitted reaction: although 20 min illumination now yielded a lower N:C ratio of 9%, this value increased to 13% when the reaction was extended to 40 min (Figure 2d). Conversely, increasing the illumination power to 80 mW/cm² did not further increase the N:C ratio of the product (Figure 2c). Instead, more vigorous bubble formation was noticed, suggesting that excessive azidyl radicals self-combined, analogous to what we observe in electrochemical azidation.²⁹

The azidated graphene next allowed click chemistry and biofunctionalization, e.g., copper-free cycloaddition with azadibenzocyclooctyne–PEG₄–biotin and subsequent conjugation with dye-labeled streptavidin (Figure 3a). Fluorescence micrographs (Figure 3b) showed spatially uniform functionalization across the graphene monolayer, with reduced signals at bilayer islands and wrinkles due to locally enhanced fluorescence quenching,⁴⁶ consistent with our previous results with electrochemically azidated graphene.²⁹ The N:C ratio of 13.5% we achieved in azidation suggests an azide (and hence biotin) functional group per ~ 0.6 nm² area of the graphene surface, substantially smaller than the size of the streptavidin tetramer ($\sim 5 \times 5$ nm²). The achievable labeling density is thus likely limited by the streptavidin size. In comparison, little fluorescence was observed for control graphene samples that were not azidated but went through the same labeling process (Figure 3c).

Our use of photoredox catalysis permitted reaction with visible light at low power levels. The ~ 10 mW/cm² light intensity, readily obtained by applying a color filter to a white lamp, is $\sim 10^7$ lower than typical approaches in which ~ 1 mW laser beams are focused into ~ 1 μm^2 spots (~ 1 mW/ μm^2 = 10^5 W/cm²) for visible-light-induced graphene photoreactions

and patterning.^{17,22–24,31,34} Although for the spontaneous polymerization of a diazonium at the graphene surface we have previously noted enhanced polymer deposition at a moderate ~ 0.5 W/cm² illumination,²¹ here the azidation reaction was not spontaneous without illumination (Figure 2ab) and was chemically defined toward the graphene surface.

Taking advantage of the low-visible-light condition of our reaction, we next achieved direct patterning of graphene functionalization through patterned illumination in the wide field, which removes the need for scanning a focused laser beam to achieve high local light intensity in previous photopatterning approaches.^{17,22–24} For an initial demonstration, using a 100 \times objective lens, we illuminated a confined region of the graphene sample in the above reactant and then fluorescently labeled the sample through click chemistry and biotin–streptavidin conjugation. Fluorescence microscopy showed a distinct polygon pattern of functionalization (Figure 4a), consistent with the field diaphragm of the microscope that defined the illuminated region at the sample. Line profiles across the polygon boundary showed exponentially decaying signals over a few micrometers (Figure 4b), attributable to limited diffusion of the locally generated azidyl radicals.

For finer patterns of specific shapes, we inserted a printed photomask into the expanded illumination beam path of a home-built wide-field microscope, thus projecting predefined illumination patterns to the sample at a 200-fold size reduction (Figure 4f and Materials and Methods). The resultant photopatterned azidation thus successfully defined line and text patterns with micrometer-sized features (Figure 4c–e).

CONCLUSION

Together, we have demonstrated a powerful yet facile approach for the photocatalytic azidation of graphene. The use of photoredox catalysis enabled efficient azidation with visible light at low power levels: We thus readily achieved azidation with blue light filtered from a white lamp, as well as photopatterning in the wide field without having to focus an intense laser beam into a tight spot. The resultant azidated graphene further enabled chemically defined derivations through click chemistry and subsequent bioconjugation. The examination of alternative photosensitizers and the possible generalization of our approach to other radical reactions for graphene and other surface and nanomaterials systems represent exciting future directions.

ASSOCIATED CONTENT

Supporting Information

The Supporting Information is available free of charge at <https://pubs.acs.org/doi/10.1021/acs.jpcc.2c07399>.

IRM, Raman spectroscopy, and electrical characterizations of graphene before and after photocatalytic azidation; XPS results of additional control samples (PDF)

AUTHOR INFORMATION

Corresponding Author

Ke Xu – Department of Chemistry, University of California, Berkeley, California 94720, United States; orcid.org/0000-0002-2788-194X; Email: xuk@berkeley.edu

Authors

Wan Li – Department of Chemistry, University of California, Berkeley, California 94720, United States; orcid.org/0000-0001-5751-3550

Yunqi Li – Department of Chemistry, University of California, Berkeley, California 94720, United States; orcid.org/0000-0001-8794-9910

Bowen Wang – Department of Chemistry, University of California, Berkeley, California 94720, United States

Complete contact information is available at: <https://pubs.acs.org/10.1021/acs.jpcc.2c07399>

Author Contributions

[†]W.L. and Y.L. contributed equally.

Notes

The authors declare no competing financial interest.

ACKNOWLEDGMENTS

We thank Matthew Erodici (Kwabena Bediako Group) for help with Raman spectroscopy. This work was supported by STROBE, a National Science Foundation Science and Technology Center under Grant No. DMR 1548924, and the Bakar Fellows Award.

REFERENCES

- Georgakilas, V.; Otyepka, M.; Bourlinos, A. B.; Chandra, V.; Kim, N.; Kemp, K. C.; Hobza, P.; Zboril, R.; Kim, K. S. Functionalization of graphene: covalent and non-covalent approaches, derivatives and applications. *Chem. Rev.* **2012**, *112*, 6156–6214.
- Chua, C. K.; Pumera, M. Covalent chemistry on graphene. *Chem. Soc. Rev.* **2013**, *42*, 3222–3233.
- Eigler, S.; Hirsch, A. Chemistry with graphene and graphene oxide—challenges for synthetic chemists. *Angew. Chem.-Int. Edit* **2014**, *53*, 7720–7738.
- Liao, L.; Peng, H.; Liu, Z. Chemistry makes graphene beyond graphene. *J. Am. Chem. Soc.* **2014**, *136*, 12194–12200.
- Criado, A.; Melchionna, M.; Marchesan, S.; Prato, M. The covalent functionalization of graphene on substrates. *Angew. Chem.-Int. Edit* **2015**, *54*, 10734–10750.
- Ambrosi, A.; Chua, C. K.; Latiff, N. M.; Loo, A. H.; Wong, C. H. A.; Eng, A. Y. S.; Bonanni, A.; Pumera, M. Graphene and its electrochemistry - an update. *Chem. Soc. Rev.* **2016**, *45*, 2458–2493.
- Bottari, G.; Herranz, M. A.; Wibmer, L.; Volland, M.; Rodriguez-Perez, L.; Guldi, D. M.; Hirsch, A.; Martin, N.; D'Souza, F.; Torres, T. Chemical functionalization and characterization of graphene-based materials. *Chem. Soc. Rev.* **2017**, *46*, 4464–4500.
- Kaplan, A.; Yuan, Z.; Benck, J. D.; Rajan, A. G.; Chu, X. S.; Wang, Q. H.; Strano, M. S. Current and future directions in electron transfer chemistry of graphene. *Chem. Soc. Rev.* **2017**, *46*, 4530–4571.
- Plutnar, J.; Pumera, M.; Sofer, Z. The chemistry of CVD graphene. *J. Mater. Chem. C* **2018**, *6*, 6082–6101.
- Daukiya, L.; Seibel, J.; De Feyter, S. Chemical modification of 2D materials using molecules and assemblies of molecules. *Adv. Phys.: X* **2019**, *4*, 1625723.
- Nandanapalli, K. R.; Mudusu, D.; Lee, S. Functionalization of graphene layers and advancements in device applications. *Carbon* **2019**, *152*, 954–985.
- Jeong, J. H.; Kang, S.; Kim, N.; Joshi, R.; Lee, G.-H. Recent trends in covalent functionalization of 2D materials. *Phys. Chem. Chem. Phys.* **2022**, *24*, 10684–10711.
- Ryu, S.; Han, M. Y.; Maultzsch, J.; Heinz, T. F.; Kim, P.; Steigerwald, M. L.; Brus, L. E. Reversible basal plane hydrogenation of graphene. *Nano Lett.* **2008**, *8*, 4597–4602.
- Hossain, M. Z.; Walsh, M. A.; Hersam, M. C. Scanning tunneling microscopy, spectroscopy, and nanolithography of epitaxial

- graphene chemically modified with aryl moieties. *J. Am. Chem. Soc.* **2010**, *132*, 15399–15403.
- (15) Li, B.; Zhou, L.; Wu, D.; Peng, H. L.; Yan, K.; Zhou, Y.; Liu, Z. F. Photochemical chlorination of graphene. *ACS Nano* **2011**, *5*, 5957–5961.
- (16) Zhang, L.; Diao, S.; Nie, Y.; Yan, K.; Liu, N.; Dai, B.; Xie, Q.; Reina, A.; Kong, J.; Liu, Z. Photocatalytic Patterning and Modification of Graphene. *J. Am. Chem. Soc.* **2011**, *133*, 2706–2713.
- (17) Lee, W. H.; Suk, J. W.; Chou, H.; Lee, J.; Hao, Y.; Wu, Y.; Piner, R.; Akinwande, D.; Kim, K. S.; Ruoff, R. S. Selective-Area Fluorination of Graphene with Fluoropolymer and Laser Irradiation. *Nano Lett.* **2012**, *12*, 2374–2378.
- (18) Wang, Q. H.; Jin, Z.; Kim, K. K.; Hilmer, A. J.; Paulus, G. L. C.; Shih, C. J.; Ham, M. H.; Sanchez-Yamagishi, J. D.; Watanabe, K.; Taniguchi, T.; et al. Understanding and controlling the substrate effect on graphene electron-transfer chemistry via reactivity imprint lithography. *Nat. Chem.* **2012**, *4*, 724–732.
- (19) Kirkman, P. M.; Güell, A. G.; Cuharuc, A. S.; Unwin, P. R. Spatial and Temporal Control of the Diazonium Modification of sp^2 Carbon Surfaces. *J. Am. Chem. Soc.* **2014**, *136*, 36–39.
- (20) Valenta, L.; Kovaricek, P.; Vales, V.; Bastl, Z.; Drogowska, K. A.; Verhagen, T. A.; Cibulka, R.; Kalbac, M. Spatially Resolved Covalent Functionalization Patterns on Graphene. *Angew. Chem.-Int. Edit* **2019**, *58*, 1324–1328.
- (21) Li, Y.; Li, W.; Wojcik, M.; Wang, B.; Lin, L.-C.; Raschke, M. B.; Xu, K. Light-assisted diazonium functionalization of graphene and spatial heterogeneities in reactivity. *J. Phys. Chem. Lett.* **2019**, *10*, 4788–4793.
- (22) Wei, T.; Al-Fogra, S.; Hauke, F.; Hirsch, A. Direct Laser Writing on Graphene with Unprecedented Efficiency of Covalent Two-Dimensional Functionalization. *J. Am. Chem. Soc.* **2020**, *142*, 21926–21931.
- (23) Edelthhammer, K. F.; Dasler, D.; Jurkiewicz, L.; Nagel, T.; Al-Fogra, S.; Hauke, F.; Hirsch, A. Covalent 2D-Engineering of Graphene by Spatially Resolved Laser Writing/Reading/Erasing. *Angew. Chem.-Int. Edit* **2020**, *59*, 23329–23334.
- (24) Bao, L.; Zhao, B.; Yang, B.; Halik, M.; Hauke, F.; Hirsch, A. Hypervalent Iodine Compounds as Versatile Reagents for Extremely Efficient and Reversible Patterning of Graphene with Nanoscale Precision. *Adv. Mater.* **2021**, *33*, No. e2101653.
- (25) Rodriguez Gonzalez, M. C.; Leonhardt, A.; Stadler, H.; Eyley, S.; Thielemans, W.; De Gendt, S.; Mali, K. S.; De Feyter, S. Multicomponent Covalent Chemical Patterning of Graphene. *ACS Nano* **2021**, *15*, 10618–10627.
- (26) Wei, T.; Hauke, F.; Hirsch, A. Evolution of Graphene Patterning: From Dimension Regulation to Molecular Engineering. *Adv. Mater.* **2021**, *33*, 2104060.
- (27) Wei, T.; Liu, X.; Kohring, M.; Al-Fogra, S.; Moritz, M.; Hemmeter, D.; Paap, U.; Papp, C.; Steinrück, H.-P.; Bachmann, J.; et al. Molecular Stacking on Graphene. *Angew. Chem.-Int. Edit* **2022**, *61*, No. e202201169.
- (28) Li, W.; Wojcik, M.; Xu, K. Optical microscopy unveils rapid, reversible electrochemical oxidation and reduction of graphene. *Nano Lett.* **2019**, *19*, 983–989.
- (29) Li, W.; Li, Y.; Xu, K. Azidated graphene: direct azidation from monolayers, click chemistry, and bulk production from graphite. *Nano Lett.* **2020**, *20*, 534–539.
- (30) Li, W.; Li, Y.; Xu, K. Facile, electrochemical chlorination of graphene from an aqueous NaCl solution. *Nano Lett.* **2021**, *21*, 1150–1155.
- (31) Liu, H. T.; Ryu, S. M.; Chen, Z. Y.; Steigerwald, M. L.; Nuckolls, C.; Brus, L. E. Photochemical reactivity of graphene. *J. Am. Chem. Soc.* **2009**, *131*, 17099–17101.
- (32) Zhang, L.; Zhou, L.; Yang, M.; Liu, Z.; Xie, Q.; Peng, H.; Liu, Z. Photo-induced free radical modification of graphene. *Small* **2013**, *9*, 1134–1143.
- (33) Liao, L.; Song, Z. H.; Zhou, Y.; Wang, H.; Xie, Q.; Peng, H. L.; Liu, Z. F. Photoinduced methylation of graphene. *Small* **2013**, *9*, 1348–1352.
- (34) Liao, L.; Wang, H.; Peng, H.; Yin, J. B.; Koh, A. L.; Chen, Y. L.; Xie, Q.; Peng, H. L.; Liu, Z. F. van Hove singularity enhanced photochemical reactivity of twisted bilayer graphene. *Nano Lett.* **2015**, *15*, 5585–5589.
- (35) Koike, T.; Akita, M. Visible-light radical reaction designed by Ru- and Ir-based photoredox catalysis. *Inorg. Chem. Front* **2014**, *1*, 562–576.
- (36) Shaw, M. H.; Twilton, J.; MacMillan, D. W. C. Photoredox Catalysis in Organic Chemistry. *J. Org. Chem.* **2016**, *81*, 6898–6926.
- (37) McAtee, R. C.; McClain, E. J.; Stephenson, C. R. J. Illuminating Photoredox Catalysis. *Trends Chem.* **2019**, *1*, 111–125.
- (38) Tay, N. E. S.; Lehnher, D.; Rovis, T. Photons or Electrons? A Critical Comparison of Electrochemistry and Photoredox Catalysis for Organic Synthesis. *Chem. Rev.* **2022**, *122*, 2487–2649.
- (39) Kwon, K.; Simons, R. T.; Nandakumar, M.; Roizen, J. L. Strategies to Generate Nitrogen-centered Radicals That May Rely on Photoredox Catalysis: Development in Reaction Methodology and Applications in Organic Synthesis. *Chem. Rev.* **2022**, *122*, 2353–2428.
- (40) Li, X. S.; Cai, W. W.; An, J. H.; Kim, S.; Nah, J.; Yang, D. X.; Piner, R.; Velamakanni, A.; Jung, I.; Tutuc, E.; et al. Large-area synthesis of high-quality and uniform graphene films on copper foils. *Science* **2009**, *324*, 1312–1314.
- (41) Liang, X.; Sperling, B. A.; Calizo, I.; Cheng, G.; Hacker, C. A.; Zhang, Q.; Obeng, Y.; Yan, K.; Peng, H.; Li, Q.; et al. Toward Clean and Crackless Transfer of Graphene. *ACS Nano* **2011**, *5*, 9144–9153.
- (42) Li, W.; Moon, S.; Wojcik, M.; Xu, K. Direct optical visualization of graphene and its nanoscale defects on transparent substrates. *Nano Lett.* **2016**, *16*, 5027–5031.
- (43) Wojcik, M.; Hauser, M.; Li, W.; Moon, S.; Xu, K. Graphene-enabled electron microscopy and correlated super-resolution microscopy of wet cells. *Nat. Commun.* **2015**, *6*, 7384.
- (44) DeFelippis, M. R.; Faraggi, M.; Klapper, M. H. Redox potentials of the azide and dithiocyanate radicals. *J. Phys. Chem.* **1990**, *94*, 2420–2424.
- (45) Wojcik, M.; Li, Y.; Li, W.; Xu, K. Spatially resolved *in situ* reaction dynamics of graphene via optical microscopy. *J. Am. Chem. Soc.* **2017**, *139*, 5836–5841.
- (46) Kim, J.; Cote, L. J.; Kim, F.; Huang, J. X. Visualizing graphene based sheets by fluorescence quenching microscopy. *J. Am. Chem. Soc.* **2010**, *132*, 260–267.